Supporting Information for:

A new orange ligand-dependent fluorescent reporter for anaerobic imaging

Hannah E. Chia[1], Karl J. Koebke[2], Aathmaja A. Rangarajan[2], Nicole M. Koropatkin[3], E. Neil G. Marsh[1,2,4], Julie S. Biteen[1,2]*

[1]Program in Chemical Biology, University of Michigan, Ann Arbor, MI 48019 USA
[2]Department of Chemistry, University of Michigan, Ann Arbor, MI 48109 USA
[3]Department of Microbiology and Immunology, University of Michigan Medical School, Ann Arbor, MI 48109 USA
[4]Department of Biological Chemistry, University of Michigan, Ann Arbor, MI 48109 USA

*Correspondence: jsbiteen@umich.edu

Contents:

Experimental Materials & Methods

Protein Expression

MBP-UnaG was prepared as previously reported[S1] and stored at 4 °C in Buffer A, consisting of filtered 20 mM Tris-HCl (pH 7.2), 200 mM NaCl, and 1 mM EDTA. MBP-UnaG is referred to as UnaG throughout the *in vitro* HTS and spectral characterization experiments.

HTS Assay Protocol

For primary assays, black, low-volume, non-coated 384-well plates (Greiner Bio-One, Ref. 784900) were prepared by dispensing 10 µL of Buffer A using a Multidrop Combi Reagent Dispenser (Thermo Scientific). Compounds were added into sample wells using a Sciclone liquid handler with a pin tool (50 nL of 2 mM stock in DMSO, 5 µM final concentration); an equivalent volume of DMSO was added to control wells. UnaG protein was subsequently dispensed into plates (10 µL of 1 mM stock, 500 nM final concentration). Negative controls were buffer-only wells and protein-only wells. Bilirubin (br) was added to positive control wells (2 µL, 5 µM final). Plates were covered with aluminum foil to prevent light exposure and incubated by shaking on the Multidrop dispenser (10 min, 500 rpm). Plates were centrifuged (1 min, 1000 rpm) before measurements.

For confirmation assays, compounds were dispensed with a Mosquito picker (50 nL of 2 mM stock in DMSO, 5 µM final; TTP Labtech); plates were prepared with Buffer A and UnaG protein as was done for the primary assays above. For secondary assays, plates were prepared similar to confirmation assays with the exception of adding 10 µL Buffer A instead of UnaG protein.

Fluorescence intensity was detected using a PHERAstar plate reader (BMG Labtech) using three optics modules centered at excitation/emission wavelengths of 485/520 nm, 540/570 nm, and 580/610 nm, respectively.

Compound libraries

All compounds screened were stored at the University of Michigan Center for Chemical Genomics. For the primary screen, 7,680 compounds from the ChemDiv 100K library were used.

Assay Performance and Data Analyses

Data collected in the 485/520 nm and 540/570 nm channels were analyzed using MScreen[S2]; data collected in the 580/610 nm channel was analyzed manually using Microsoft Excel.

In primary assays, compounds incubated with protein that displayed fluorescence intensity greater than ≥ 3 standard deviations (SD) away from the mean of the negative controls were considered as initial hits. Compounds that fluoresced in the 540/570 nm optics module but not in the 485/520 nm module were considered preliminary hits; the same analysis was used to identify preliminary hits that fluoresced in the 580/610 nm module but not 485/520.

In confirmation and secondary assays, preliminary hits were evaluated in triplicate. Compounds incubated with protein that exhibited an increase in fluorescence intensity greater than ≥ 3 SD from the mean of the negative controls were considered hits in confirmation assays. However, these compounds were excluded from the final hit list if the compound-only plates in secondary screening also produced fluorescence intensity greater than ≥ 3 SD from the mean of the negative controls. Compounds that were hits in primary and confirmation assays but not in secondary assays were considered confirmed hits and ordered from MolPort (Table S3). These confirmed hits were analyzed in concentration-dependent curves in duplicate.

Spectral Characterization and Titrations

UnaG and compounds were all prepared for measurements in Buffer A. UV-Visible absorbance measurements were performed in 96-well clear bottom plates using the Molecular Devices SpectraMax iD3 microplate reader or in a black-walled quartz cuvette (Hellma, 1 cm pathlength) using a Hewlett Packard 8453 UV-vis spectrophotometer. Molar extinction coefficient (ε) was calculated using the Beer-Lambert law. Plotted UV-vis spectra are background corrected using buffer blanks and processed using MATLAB.

Fluorescence measurements were carried out on an Agilent Varian Cary Eclipse Fluorescence Spectrophotometer. Plotted fluorescence excitation and emission spectra are averaged plots from three technical replicates.

Fluorescence titrations were performed by taking fluorescence emission spectra at 495-nm excitation of UnaG bound with br, followed by parallel additions of competing ligand to a br-only sample and competing ligand to the UnaG-br complex. After each addition of competing ligand, the sample was allowed to equilibrate for 10 min before fluorescence measurements[S3]. The compound-only spectra were used for background subtraction for competing ligand-UnaG-br readings. Assuming a 1:1 displacement of br by the competing ligand, the concentration of free competing ligand was calculated to use for fitting. Data was fit using Prism (GraphPad) using a single-site binding model with a linear baseline correction:

$$\mathrm{Y} = \mathrm{C} + \mathrm{S}\,[\mathrm{L}] + \frac{\mathrm{B_{max}}\,[\mathrm{L}]}{\mathrm{K_{d(app)}} + [\mathrm{L}]}$$

Where *Y* is the signal of the UnaG-br complex, and *[L]* is the concentration of the competing ligand, *C* and *S* are intercept and slope of the baseline, B_{max} is the fluorescence in the absence of *L*, and $K_{d(app)}$ is the apparent dissociation constant of L. $K_{d(app)}$ was corrected to the true K_d for *L* using the known K_d for br as described in the supporting information.

Cell Cultures

The *B. ovatus* and *B. theta* strains used in this study have been previously described[S1]. *B. ovatus* and *B. theta* strains were initially started in rich media containing tryptone-

yeast extract-glucose and incubated anaerobically at 37 ºC in a Coy chamber. Cultures were subsequently back-diluted into minimal media with 0.05% w/v maltose as a carbohydrate source.

E. coli (NEBExpress, New England Biolabs) was transformed with puc19 or pMAL_c5x_UnaG plasmids using standard high-efficiency transformation protocols and plated on LB/Agar plates with ampicillin (amp, final 100 µg/mL). Colonies were picked into liquid LB cultures with amp to grow overnight at 37 ºC on a shaker. Cultures were subsequently back-diluted 1:200 into LB with amp to grow on a shaker at 37 ºC.

Growth Curves

B. theta cells were cultured into minimal media with 0.05% w/v maltose and back-diluted 1:200 into 96-well clear bottom plates with media and respective compounds. Each growth experiment condition was performed in triplicate. Plates were loaded into a Biostack automated plate-handling device (BioTek Instruments). Absorbance at 600 nm (OD_{600}) was measured in each well every 20 minutes by a Powerwave HT absorbance reader (BioTek Instruments). Data was recorded using Gen5 software (BioTek Instruments) and processed using Prism (GraphPad).

Fluorescence Microscopy

E. coli cells were grown to OD_{600} ~0.4 and induced with 0.4 mM IPTG to grow for 3 hours before imaging. *B. ovatus* and *B. theta* cells were grown to early to mid-log phase and imaged. For labeling with **2** and **4**, cells were incubated with a final ligand concentration of 2.5 µM for 2.5-3 hours before washing or directly used for imaging. For IFP2.0-labeled cells, bv was directly supplemented into the overnight culture (2.5 µM final concentration).

All imaging was performed at room temperature and anaerobically on cells sealed between coverslips with epoxy as previously described by our lab[S4]. Imaging was performed in an Olympus IX71 inverted epifluorescence microscope with a 100× 1.4 N.A. wide-field oil-immersion objective. Samples were illuminated by 532-nm laser (CrystaLaser CL-532-025-O; 2 mW/cm^2) or a 640-nm laser (Coherent CUBE 640-40C; 80 W/cm^2). Fluorescence emission was filtered with appropriate filter sets and imaged on a 512 × 512 pixel Andor iXon EMCCD camera at 100 frames/s. For consistency and noise reduction, all phase-contrast and fluorescence images were created by summing frames for a total of 400 ms integration time. Recorded images were analyzed using ImageJ; all images are presented on the same color scale.

Supporting References

(S1) Chia, H. E.; Zuo, T.; Koropatkin, N. M.; Marsh, E. N. G.; Biteen, J. S. Imaging Living Obligate Anaerobic Bacteria with Bilin-Binding Fluorescent Proteins. *Current Research in Microbial Sciences* **2020**, *1*, 1–6. https://doi.org/10.1016/j.crmicr.2020.04.001.

(S2) Zhang, J.-H.; Chung, T. D. Y.; Oldenburg, K. R. A Simple Statistical Parameter for Use in Evaluation and Validation of High Throughput Screening Assays. *J Biomol Screen* **1999**, *4* (2), 67–73. https://doi.org/10.1177/108705719900400206.

(S3) Jacob, R. T.; Larsen, M. J.; Larsen, S. D.; Kirchhoff, P. D.; Sherman, D. H.; Neubig, R. R. MScreen: An Integrated Compound Management and High-Throughput Screening Data Storage and Analysis System. *J Biomol Screen* **2012**, *17* (8), 1080–1087. https://doi.org/10.1177/1087057112450186.

(S4) Karunatilaka, K. S.; Cameron, E. A.; Martens, E. C.; Koropatkin, N. M.; Biteen, J. S. Superresolution Imaging Captures Carbohydrate Utilization Dynamics in Human Gut Symbionts. *mBio* **2014**, *5* (6), e02172-14. https://doi.org/10.1128/mBio.02172-14.

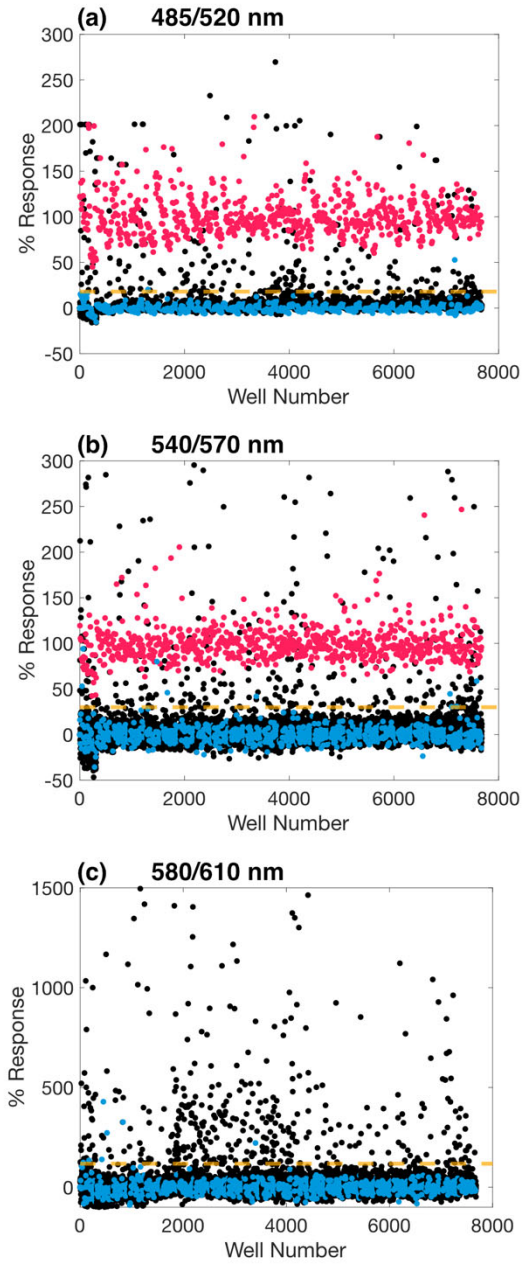

Fig. S1. Scatter plots of the entire primary high-throughput screen (HTS). Fluorescence endpoint readings were taken at (a) 485-nm excitation, 520-nm emission (485/520 nm), (b) 540-nm excitation, 570-nm emission (540/570 nm), and (c) 580-nm excitation, 610-nm emission (580/610 nm). Each dot plotted represents the percent response of a well containing a test compound (black), negative control of buffer or protein only (blue), or positive control of UnaG with bilirubin (red); the positive control exhibited no signal in the 580/610 nm module and is thus omitted in the plot in (c). Preliminary hits were selected based on signal above the 3 × SD threshold cutoff (yellow dashed line).

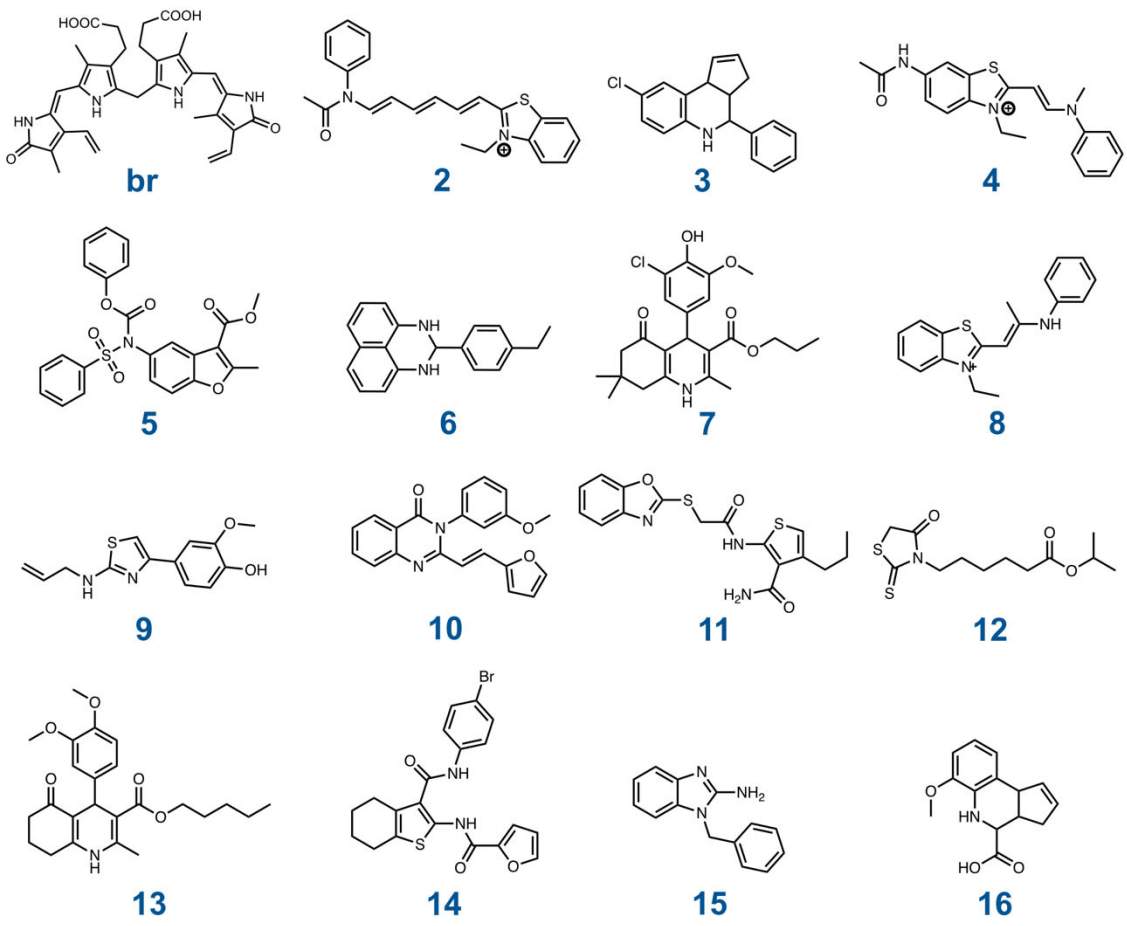

Fig. S2. Structures of the native UnaG ligand bilirubin (br) and the compounds obtained through HTS (**2**-**16**).

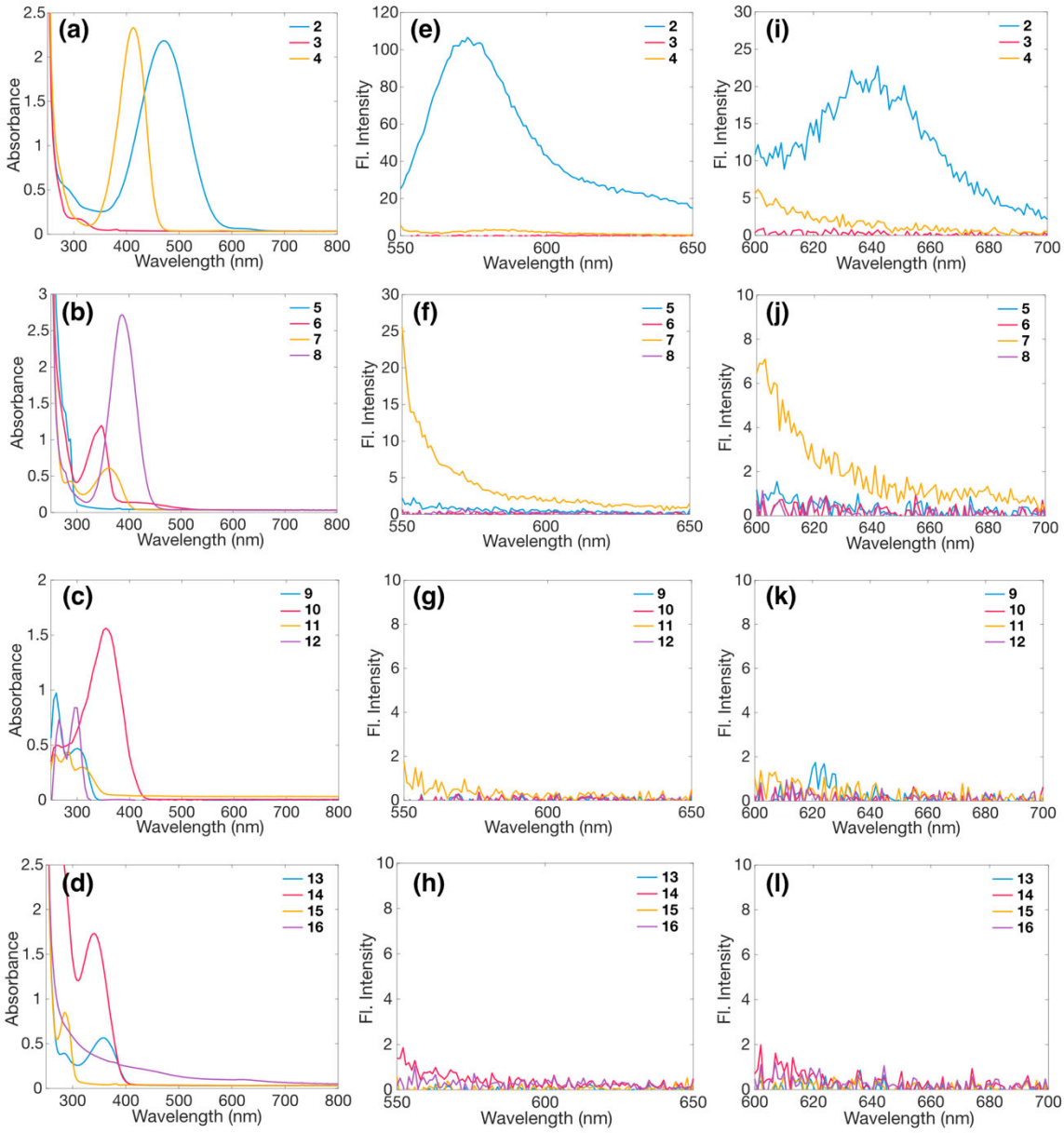

Fig. S3. (a-d) UV-vis absorbance spectra and (e-l) fluorescence emission spectra of compounds obtained through HTS. UV-vis spectra were collected in DMSO at concentration of 100 μM. Fluorescence emission of compounds in buffer were recorded from (e-h) 540-nm excitation and (i-l) 580-nm excitation at concentration of 1 μM.

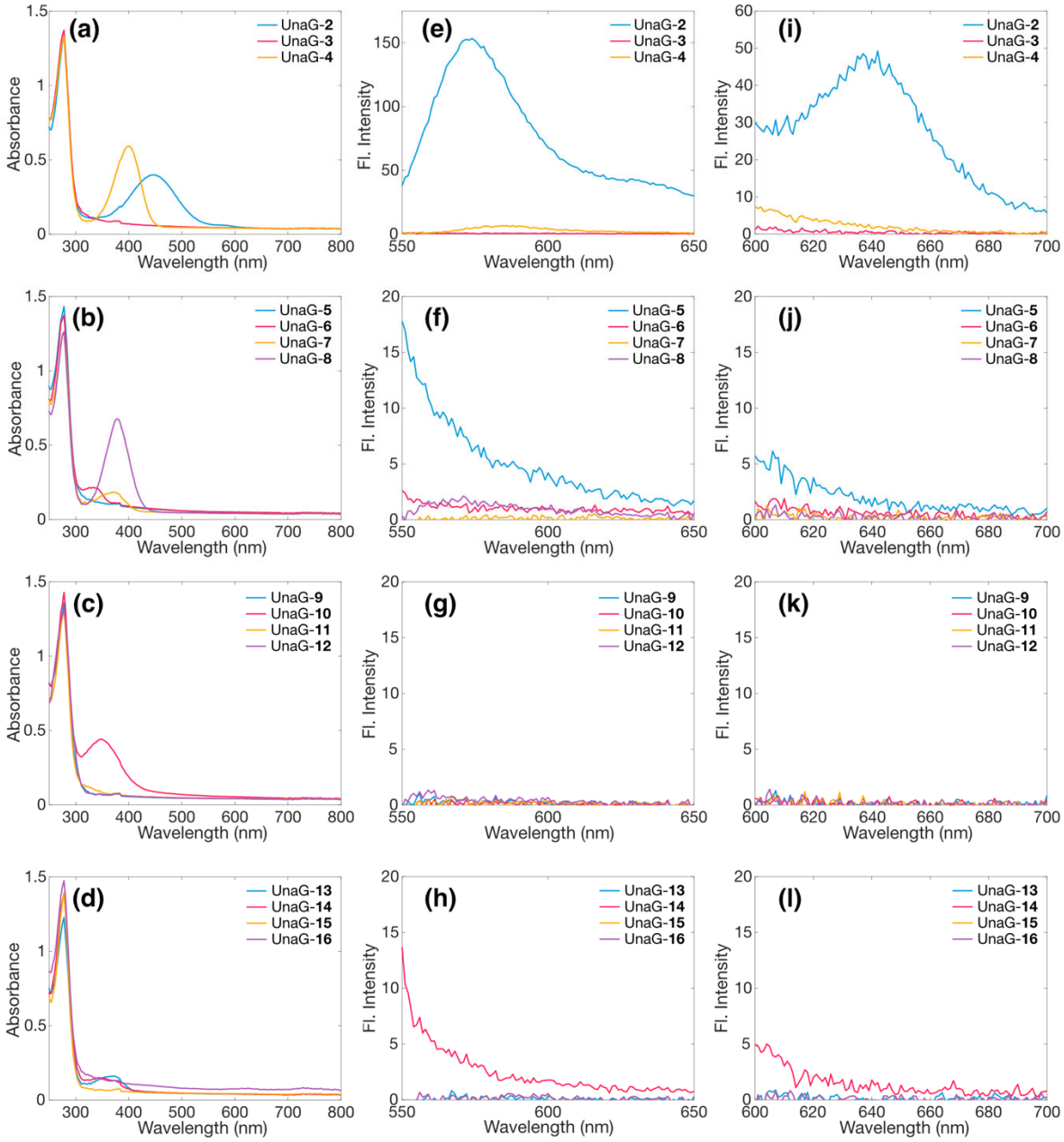

Fig. S4. (a-d) UV-vis absorbance spectra and (e-l) fluorescence emission spectra of compounds obtained through HTS incubated with UnaG. UV-vis spectra were collected in buffer at concentration of 20 μM. Fluorescence emission of UnaG-ligands in buffer were recorded from (e-h) 540-nm excitation and (i-l) 580-nm excitation at concentration of 2 μM for ligands and 100 nM for UnaG.

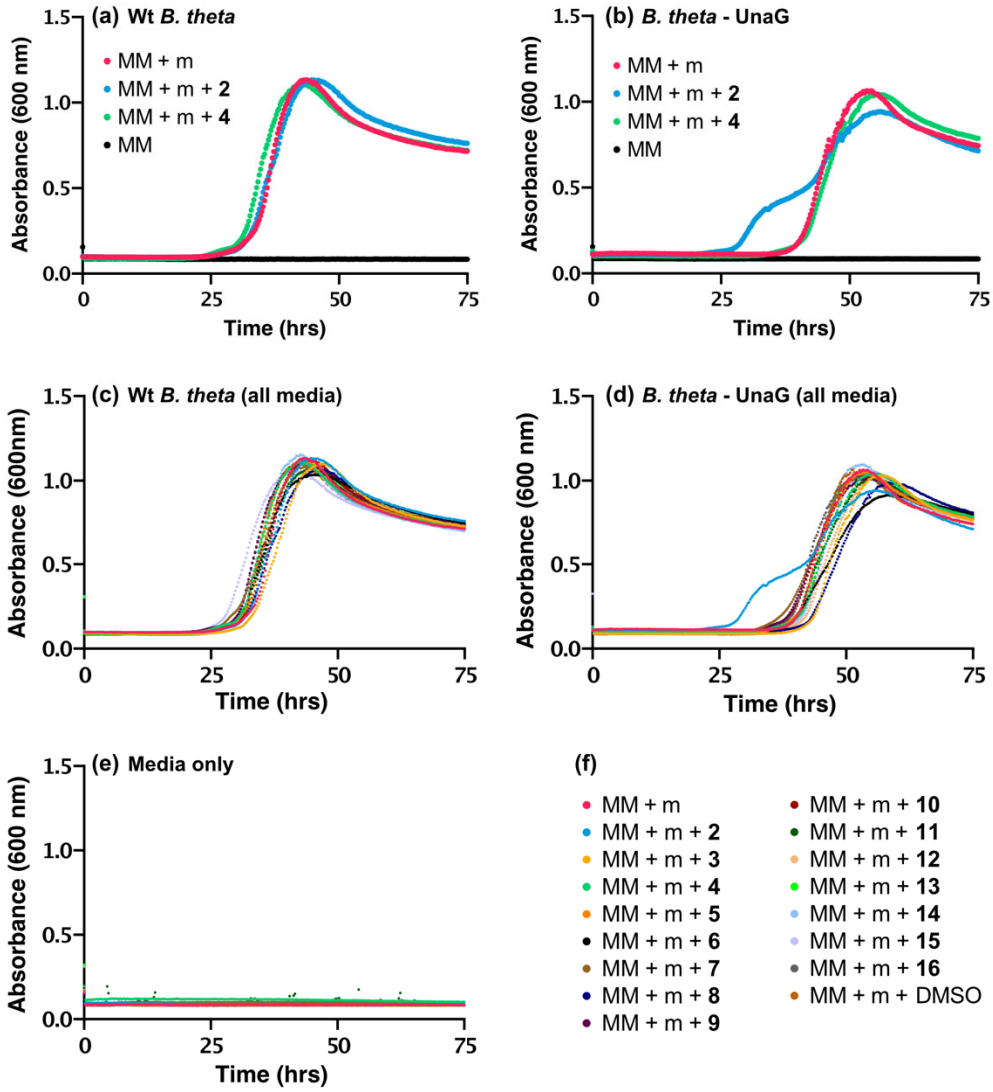

Fig. S5. Growth measured by absorbance (600 nm) for cells grown in minimal media (MM) containing 5 mg/mL maltose (m) and supplemented with 2.5 μM compounds selected from the ligand-screening process. (a) Wild-type *B. theta* and (b) *B. theta* cells expressing UnaG are unaffected by the presence of **2** and **4**, with the exception of *B. theta* - UnaG which exhibited a slight rapid growth phase in the presence of **2**. The addition of compounds **2 – 16** as well as 0.005% DMSO does not affect the growth of (c) Wt *B. theta*, (d) *B. theta* - UnaG, or (e) media-only conditions. (f) strain legend for panels c-e.

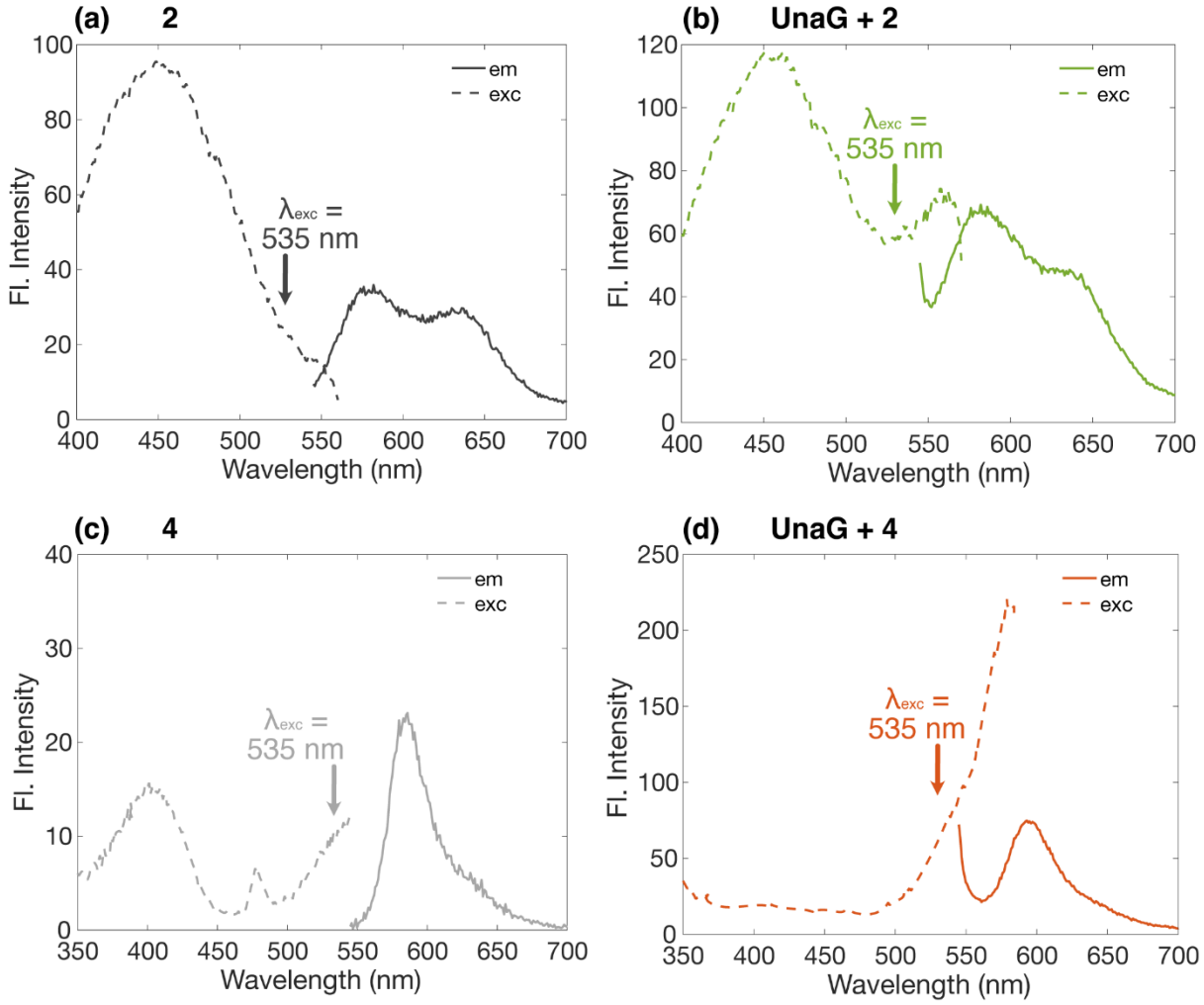

Fig. S6. Fluorescence excitation (exc) and emission (em) spectra of (a) **2**, (b) UnaG incubated with **2**, (c) **4**, and (d) UnaG incubated with **4**. The fluorescence excitation wavelength, λ_{exc}, is indicated with an arrow. (a) **2** and (b) UnaG-**2** were measured at 5 μM in buffer; (c) **4** and (d) UnaG-**4** were measured at 15 μM in buffer.

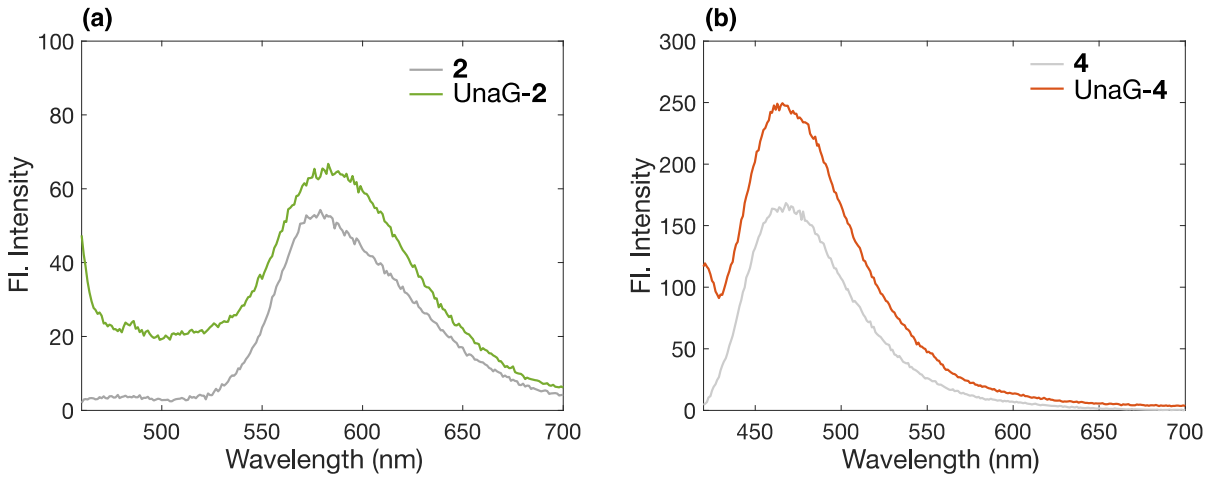

Fig. S7. Fluorescence emission spectra of (a) **2** and UnaG-**2** (5 μM) excited at 450 nm and (b) **4** and UnaG-**4** (15 μM) excited at 405 nm. All spectra were measured in buffer.

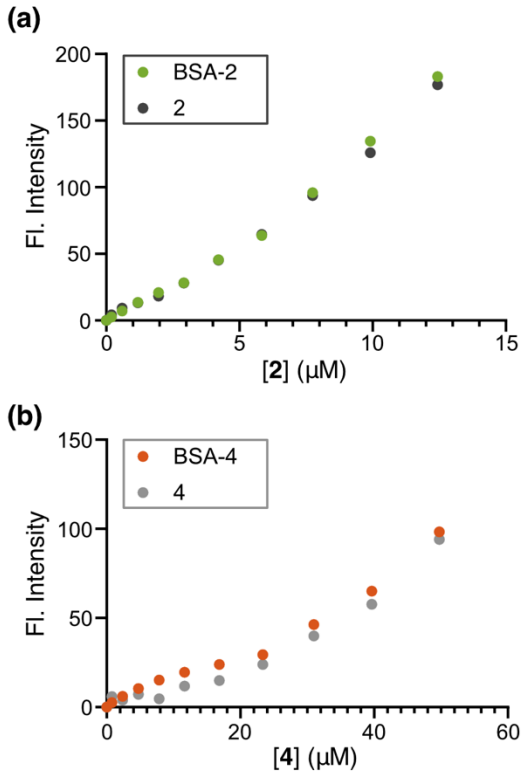

Fig. S8. Titration of BSA with (a) **2** and (b) **4**; fluorescence emission spectra were taken at 535-nm excitation and the peak emission intensities (580 nm or 596 nm) were plotted. BSA concentration were (a) 5 μM and (b) 15 μM.

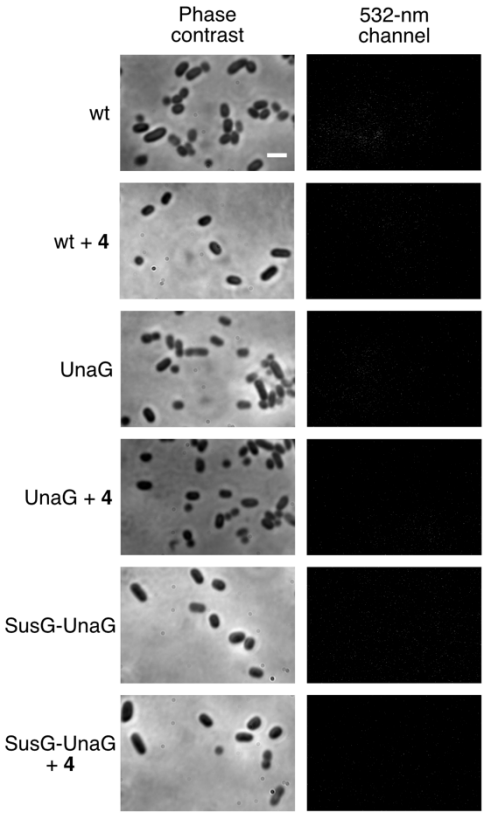

Fig. S9. (Left) phase-contrast and (right) fluorescence images of wild-type (wt) *B. theta* and *B. theta* cells expressing UnaG or SusG-UnaG and grown to mid-log phase before incubation with **4**. Cells were illuminated with 532-nm excitation. The addition of **4** did not yield any fluorescence signal from UnaG-labeled cells. Scale bar: 2 μm.

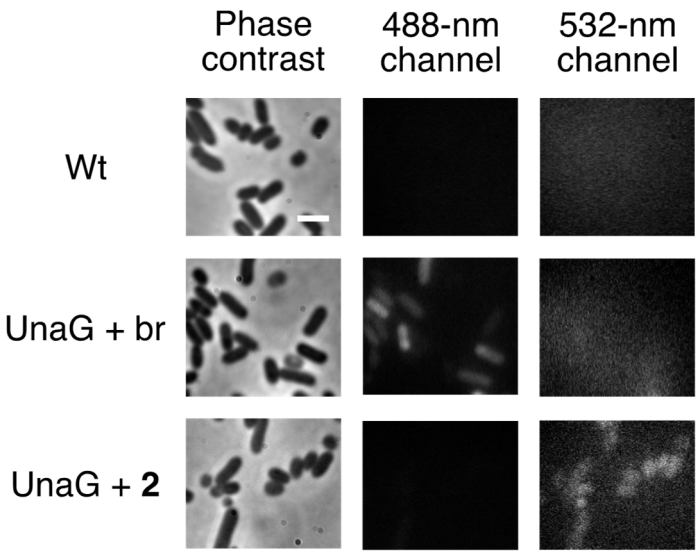

Fig. S10. To evaluate ligand and excitation specificity, *B. theta* expressing UnaG were grown with br or incubated with **2** and excited by 488-nm or 532-nm illumination. *B. theta* cells expressing UnaG grown with br are only fluorescent in the 488-nm channel, while cells incubated with **2** are only fluorescent in the 532-nm channel. Images presented in each laser channel are presented on the same intensity scale. Scale bar: 2 μm.

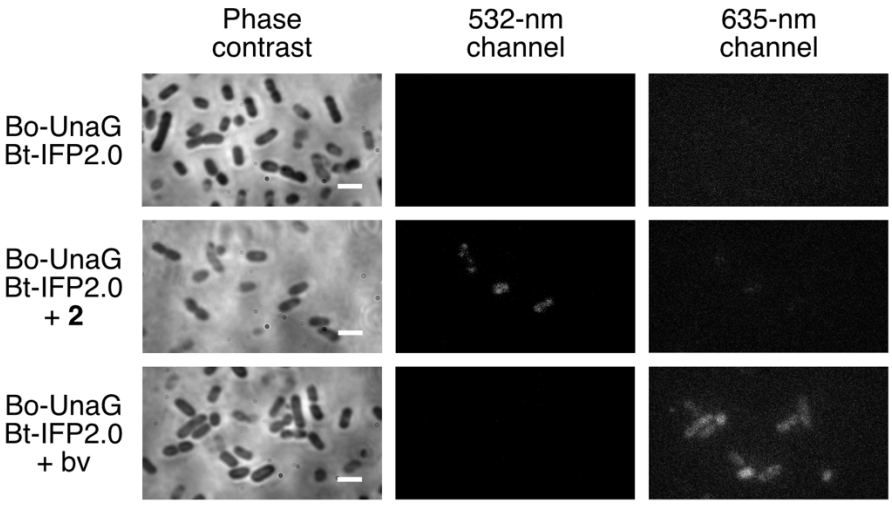

Fig. S11. Phase-contrast and fluorescence images of *B. ovatus* (*Bo*) expressing UnaG and *B. theta* (*Bt*) expressing IFP2.0. When **2** is supplemented into media for labeling or when cells are grown in bv, UnaG-labeled *B. ovatus* can be distinguished from IFP2.0-labeled *B. theta* in separate color channels using 532-nm and 635-nm excitation, respectively. Scale bar: 2 μm.

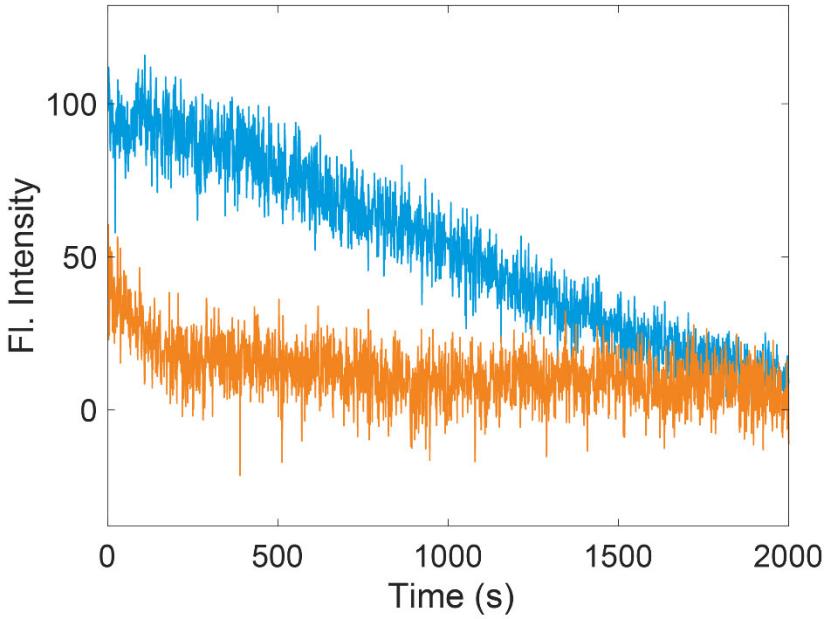

Fig. S12. Fluorescence intensity decay of UnaG-labeled *B. theta* cells incubated with br (blue, 488-nm excitation, 10 W/cm^2) and **2** (orange, 532-nm excitation, 4 W/cm^2) under constant illumination. Using the background-subtracted fluorescence intensity of a single cell normalized to cell area, the average fluorescence intensity from five representative cells is plotted per condition.

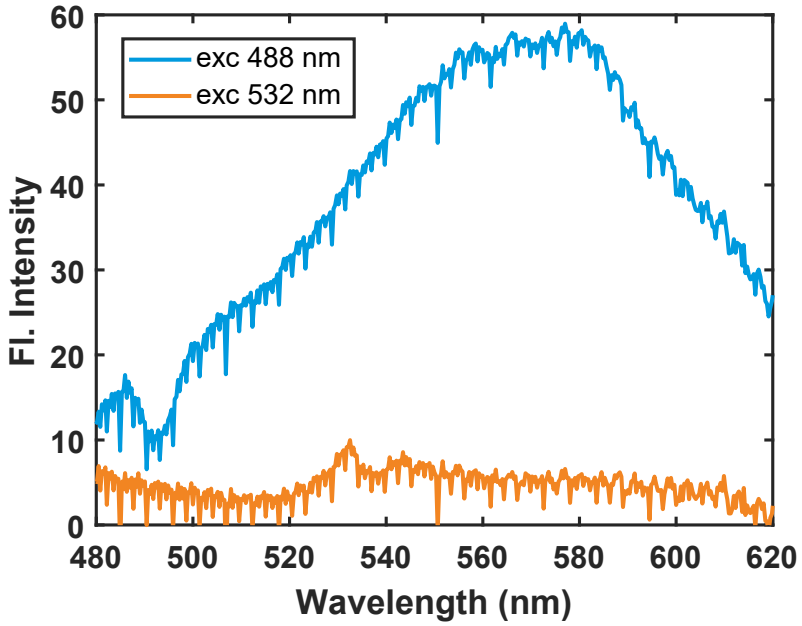

Fig. S13. Fluorescence spectra of wt *B. theta* cells under excitation at 488-nm (blue) and at 532-nm (orange). The excitation power is the same (3mW) for both sources and each curve is the average of the spectra for five cells.

Table S1. Extinction coefficients of confirmed hit compounds and compounds bound to UnaG at the excitation wavelength of 535 nm.

	ε (M^{-1} cm^{-1}) at 535 nm
2 alone	15349
UnaG - **2**	82362
4 alone	13918
UnaG - **4**	25379

Supplemental Discussion

Determination of K_d for compounds 2 and 4 through competitive binding experiments from $K_{d\ (app)}$

The K_ds for compounds **2** and **4** were determined by following the decrease in fluorescence as the compounds were titrated against a fixed concentration of UnaG and br (50 nM of protein and ligand for compound **2** and 25 nM of protein and ligand for compound **4**). The titration curves (show in the main text) were fitted to a simple binding isotherm which provides the apparent K_d for **2** and **4** in the presence of a fixed concentration of br. For a competitive binding model, the relationship between $K_{d,c}$ and $K_{d(app)}$ is given by equation (1):

$$K_{d\ (app)} = K_{d,c}\left(1 + \frac{L_{br,free}}{K_{d,br}}\right) \quad (1)$$

Where $K_{d\ (app)}$ is the experimentally determined dissociation constant and $K_{d,c}$ is the true disassociation constant for the titrated competitor ligand; $K_{d,br}$ is the disassociation constant for br binding to UnaG, which was measured as 3 nM and $L_{br,free}$ is the *free* concentration of br in solution.

To determine the free concentration $L_{br,free}$, we calculated the concentration of the UnaG-br complex (EL_{br}) from the known, total UnaG concentration (E_t) and total br concentration (L_t) using the following standard relationships:

$$E + L_{br} \rightleftharpoons EL_{br}$$

$$K_{d,br} = \frac{(E_{free})(L_{br,free})}{EL_{br}}$$

$$K_{d,br} = \frac{(E_t - EL_{br})(L_t - EL_{br})}{EL_{br}}$$

$$EL_{br} = \frac{E_t + L_t + K_{d,br} \pm \sqrt{E_t^2 - 2E_tL_t + 2E_tK_{d,br} + L_t^2 + K_{d,br}^2 + 2L_tK_{d,br}}}{2} \quad (2)$$

Equation (2) was solved to find the equilibrium concentration of the UnaG-br complex and hence the free concentration of br. This value was used in Equation (1) to correct the apparent K_d to calculate the true K_d.

Table S2. The calculated $K_{d(app)}$ and true K_d from fluorescence competition titrations for **2** and **4**.

Compound	$K_{d(app)}$ nM	K_d (nM)
2	13 ± 4	3
4	35 ± 8	10

Table S3. Compounds ordered from MolPort, Inc. for concentration-dependent screening.

ID in this study	Hit in HTS channel	MolPort ID	Catalog No.	Supplier
2	540/570	MolPort-035-896-678	4090-1986	ChemDiv, Inc.
3	580/610	MolPort-001-836-754	1959-0257	ChemDiv, Inc.
4	580/610	MolPort-047-118-081	0898-0008	ChemDiv, Inc.
5	540/570	MolPort-000-564-975	AG-690/12510375	Specs
6	580/610	MolPort-000-445-083	AG-690/12890124	Specs
7	580/610	MolPort-001-931-262	AG-690/10379022	Specs
8	540/570	MolPort-000-717-433	STK874239	Vitas-M Laboratory, Ltd.
9	540/570	MolPort-001-965-798	STK831400	Vitas-M Laboratory, Ltd.
10	580/610	MolPort-001-848-862	STK094419	Vitas-M Laboratory, Ltd.
11	580/610	MolPort-001-004-902	STK039750	Vitas-M Laboratory, Ltd.
12	540/570	MolPort-000-225-490	STK396289	Vitas-M Laboratory, Ltd.
13	580/610	MolPort-001-931-334	STK372609	Vitas-M Laboratory, Ltd.
14	540/570	MolPort-001-935-437	STK084537	Vitas-M Laboratory, Ltd.
15	540/570	MolPort-002-116-650	STK094803	Vitas-M Laboratory, Ltd.
16	580/610	MolPort-001-951-131	STK893803	Vitas-M Laboratory, Ltd.